Heterodimeric Molecules Including Nucleic Acid Bases and 9-Aminoacridine. Spectroscopic Studies, Conformations, and Interactions with DNA

Jean F. Constant,[‡,§] Philippe Laûgaa,[∥] Bernard P. Roques,[∥] and Jean Lhomme*[,‡,§]

Chimie Organique Biologique, Université de Lille I, UA CNRS 351, 59655 Villeneuve d'Ascq Cêdex, France, and Departement de Chimie, Université R. Descartes, UA CNRS 613, 75270 Paris Cêdex 06, France

Received August 4, 1987; Revised Manuscript Received December 16, 1987

ABSTRACT: Heterodimeric molecules have been examined in which the 9-amino-6-chloro-2-methoxyacridine ring is linked to the nucleic acid bases adenine, thymine, and guanine by polymethylenic chains $(CH_2)_n$ of varying length (n = 3, 5, 6). A detailed analysis has been performed, including hypochromism measurement in the UV, chemical shift variations in Fourier transform proton magnetic resonance, and fluorescence emission. All these techniques show that all molecules exist mainly under folded conformations in water in the temperature range 0–90 °C, with the acridine and the base rings being stacked one on top of the other. The thermodynamic parameters for the folded ⇌ unfolded conformational equilibrium were estimated. The geometry of the intramolecular complexes could be determined. (1) All these data give information on the strength and nature of the base–acridine interactions as a function of different parameters such as solvent, temperature, etc. (2) The molecules under study constitute "spectroscopic models" for the drug–base complexes as they occur in DNA. In particular, we show the dramatic influence of the relative orientations of the two stacked chromophores in the complex upon the magnitude of % H, the percent hypochromism. The quenching and enhancement of acridine fluorescence emission induced respectively by guanine and adenine is evidenced and quantitatively estimated. (3) These base–acridine heterodimers bind to DNA to an extent that is inversely proportional to their degree of intramolecular stacking.

Quinacrine (**1**) is an antimalarial drug that inhibits the DNA replication and RNA transcription in susceptible cells (Hahn, 1978; Thompson, 1972). In vitro it forms reversible complexes of the intercalation type with polynucleotides, in which the protonated amino aliphatic side chain interacts ionically with the phosphate groups of the polymer, while ring–ring stacking interactions are involved between the protonated acridine ring of the drug and the nucleotide bases (Waring, 1970, 1975; Georghiou, 1977; Patel, 1977).

In a general program aimed at understanding the interactions (and reactions) between intercalating drugs and the nucleic acid bases, we have prepared and examined a number of model compounds in which the aromatic part of the drug is linked to the base by a three methylene bridge, which allows an intramolecular ring–ring stacking interaction (or reaction). The position of the equilibrium between the folded and unfolded forms in aqueous solution, as determined by UV and NMR experiments, was used as a measure of the interaction. We have thus shown that in water quinolines (Bolte et al., 1976, 1977a,b, 1979, 1980), proflavin (Constant et al., 1987), and furocoumarins (Dêcout & Lhomme, 1981, 1983) associate to varying extent with the nucleic bases. In the case of furocoumarins a highly regio- and stereoselective photoreaction with the associated thymine base was observed as a consequence of folding (Dêcout et al., 1984).

The strongest interactions have been observed in the acridine series. The model compound in which the acridine ring of quinacrine is linked to adenine by a trimethylene bridge Ade–C_3–Acr[1] (**2a**) exists totally as folded conformations in water (Bolte et al., 1982). Total folding was still observed at 80 °C. This shows the dramatic contribution of ring–ring stacking interactions in binding processes. From this observation we have prepared (Constant et al., 1985) new molecules, which are described in this paper (Chart I). These compounds attach the three bases adenine (**2b,c**), thymine (**3b,c**), and guanine (**4b,c**) to a quinacrine ring by either a C_5 or C_6 chain. The degree of stacking in water and the geometries of the intramolecular complexes could be determined by using UV, ^{1}H NMR, and fluorescence spectroscopies. With these "spectroscopic models" experimental evidence is obtained for the dramatic influence of the geometry of the complex upon the magnitude of hypochromic effects. Fluorescence emission is shown to be very sensitive to the nature of the attached base. The binding properties of these new molecules have been determined by measurement of the association constants with DNA.

Materials and Methods

Materials. The following compounds have been prepared and described before: Ade–C_3 (**6**), Thy–C_3 (**7**), and Gua–C_3 (**8**) (Brown et al., 1968; Leonard et al., 1969); Ade–C_3–Acr (**2a**), Thy–C_3–Acr (**3a**), and Acr–C_3 (**5**) (Bolte et al., 1982); Ade–C_5–Acr (**2b**), Ade–C_6–Acr (**2c**), Thy–C_5–Acr (**3b**), Thy–C_6–Acr (**3c**), Gua–C_5–Acr (**4b**), and Gua–C_6–Acr (**4c**) (Constant et al., 1985). All compounds were tested for purity by a variety of methods including microanalysis, ^{1}H NMR spectroscopy, thin-layer chromatography, and high-performance liquid chromatography (HPLC) in different solvent systems.

UV Spectroscopy. The quantitative ultraviolet spectrometric measurements were made with a Beckman Acta M 5270

* Address correspondence to this author at the Université de Grenoble.
‡ Université de Lille.
§ Present address: Departement de Chimie, LEDSS, Université de Grenoble I, UA CNRS 322, BP 68, 38402 Saint Martin d'Hères, France.
∥ Université R. Descartes.

[1] Abbreviations: Ade, aden-9-yl; Thy, thym-1-yl; Gua, guan-9-yl; Acr, (6-chloro-2-methoxyacridin-9-yl)amino; Qui, (7-chloroquinolin-4-yl)-amino; C_3, *n*-propyl; C_5, *n*-pentyl; C_6, *n*-hexyl [according to the IUPAC–IUB Commission (1970) symbols and to the symbols proposed by Conn et al. (1974)]; Tris, tris(hydroxymethyl)aminoethane; EDTA, ethylenediaminetetraacetic acid.

0006-2960/88/0427-3997$01.50/0

Chart I: Structure of the Base–C_n–Acr Models and of the Corresponding Reference Compounds

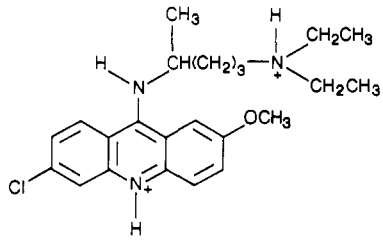

1, quinacrine

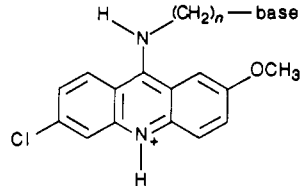

2a–c, Ade–C_n–Acr (base = 9-adenyl)
3a–c, Thy–C_n–Acr (base = 1-thymyl)
4a–c, Gua–C_n–Acr (base = 9-guanyl)

a, $n=3$; b, $n=5$; c, $n=6$

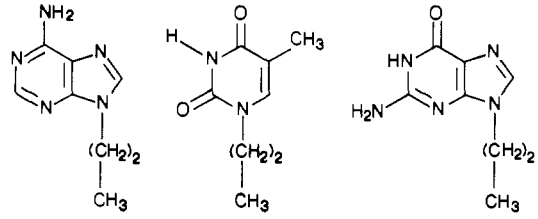

6, Ade–C_3 7, Thy–C_3 8, Gua–C_3

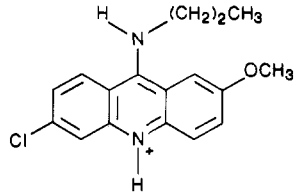

5, Acr–C_3

spectrometer as described previously (Bolte et al., 1976, 1977a,b) using dilute aqueous solutions. Spectral grade ethanol (Prolabo) and deionized bidistilled water were used.

Samples of each compound were dissolved in absolute ethanol and then diluted with water to give (2–8) × 10^{-5} M solutions containing 5% ethanol and showing a maximum optical density of 0.8 (Beer's law was obeyed in this range).

The solution was adjusted to pH 5.5 by using acetate buffer (0.05 M) to ensure total protonation of the acridine ring. Spectra were determined in 10-mm cells.

The hypochromic effect is quantitatively expressed by the percent hypochromism (% *H*). It was calculated according to the equation

$$\% H = 1 - (\mathcal{F}B\text{–}C_3\text{–}Acr)/(\mathcal{F}B\text{–}C_3 + \mathcal{F}Acr\text{–}C_3)$$

where $\mathcal{F}$ is the oscillator strength of the transition, i.e., a measure of the intensity of the absorption: $\mathcal{F} = (4.32 \times 10^{-9}) \int \epsilon(\lambda)/\lambda^2 \, d\lambda$, where ϵ is the molecular extinction coefficient. The $\mathcal{F}$ values were obtained from optical densities measured every 2.5 nm by application of the Simpson rule. We calculated % *H* in the 360–500-nm region of the spectrum, where the bases do not absorb; i.e., the term B–C_3 is suppressed in the calculation of % *H*.

^1H NMR Studies. ^{1}H NMR spectra were recorded at 270 MHz (Bruker WH 270) or 400 MHz (Bruker AM 400) operating in the Fourier transform mode and locked to the deuterium resonance of the solvent D_2O. Stock solutions of the studied compounds were made in a deuterioacetate buffer (0.04 M, pD 5.5). Probe temperature was regulated to ±1 °C by a Bruker BST 100/700 controller.

Fluorescence Studies. Fluorescence emission spectra were recorded with a FICA 55000 spectrofluorometer. The concentrations of the studied compounds (non-degassed solutions, buffered as for the UV measurements) were chosen for an optical density smaller than 0.04 at the excitation wavelength (360 nm). A spectral width of 7.5 mm was used.

For determination of the quantum yields of fluorescence we used a solution of quinine bisulfate in 1 N sulfuric acid as a standard (Birks, 1976). We also corrected for the refraction indices of the solvents.

DNA Binding Studies. DNA binding studies were performed with a Perkin-Elmer MPF-44A spectrofluorometer in a thermostated quartz cell (25 °C). Excitation and emission were monitored at the ethidium bands (520, 600 nm).

All solutions were made in 25 mM Tris-HCl, pH 7, 0.1 M NaCl, and 0.2 mM EDTA containing derivatives. The DNA binding parameters have been checked in these conditions. The DNA concentration was 1.6 × 10^{-5} M (in base pairs) and that of model compounds 2 × 10^{-5} M.

Results and Discussion

The ring–ring intramolecular properties of the models were investigated by hypochromism measurement in the UV, high-field ^{1}H NMR spectroscopy, and fluorescence emission.

UV Studies

The binding of quinacrine to DNA and synthetic polynucleotides has been thoroughly studied by examining the UV spectrum of the drug molecule in the presence of the relevant polynucleotide (Krey & Hahn, 1974, 1975; Nastasi et al., 1976). Intercalation of the acridine moiety of the drug between the nucleotide bases results in a strong decrease of the absorption intensity of the quinacrine chromophore ("hypochromic effect") accompanied by a slight shift to the blue in the region of the absorption maximum. We therefore selected this method to detect the ring–ring interaction in our models and to compare the results with those reported for drug–DNA interactions. In addition, the value (and the limits) of this hypochromism technique to assess stacking interactions has been amply demonstrated, notably by N. J. Leonard [see for review, Leonard (1979)] in a series of nucleic acid bases and coenzymes. We have also used it to evaluate the interaction between different intercalators, aminoquinolines, acridines, furocoumarins, and nucleotide bases (Bolte et al., 1982; Décout & Lhomme, 1983; Constant et al., 1987). The absorption spectra of all the models base–C_n–Acr were recorded and compared with that of the monomer Acr–C_3 (**5**), measured at the same concentration. All exhibit a strong decrease in the absorption and a shift to long wavelengths, as observed for quinacrine intercalated in DNA. The % *H* values for the different model compounds are given in Table I. Comparison of the different systems indicate that (1) for a given chain length % *H* is higher in the purine series than for the thymine models and (2) for a given base % *H* is strongly influenced by the chain length. It decreases when *n* increases.

However, this direct comparison cannot be quantitatively interpreted in terms of folding of the corresponding models since the magnitude of % *H* is not only dependent on the degree of stacking but also on the orientation of the transition moments of the chromophores (Devoe & Tinoco, 1962; Cantor & Schimmel, 1980). The influence of temperature on % *H* was thus examined to put the comparison on a more quanti-

Table I: Computed Percent Hypochromism (% H) for the 360–500-nm Absorption Band of Model Compounds at 25 °C (95% Water–5% Ethanol, Acetate Buffer, pH 5.5)

compound	% H	compound	% H
Ade–C_3–Acr (**2a**)	20	Thy–C_3–Acr (**3a**)	14
Ade–C_5–Acr (**2b**)	13	Thy–C_5–Acr (**3b**)	8
Ade–C_6–Acr (**2c**)	7	Thy–C_6–Acr (**3c**)	6
Gua–C_5–Acr (**4b**)	14		
Gua–C_6–Acr (**4c**)	13		

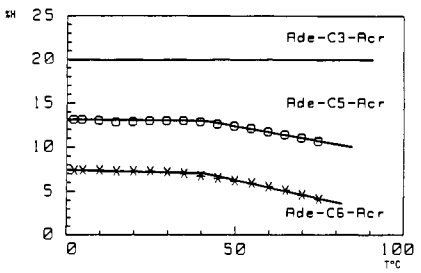

FIGURE 1: Variation of the percent hypochromism (% H) with temperature for Ade–C_3–Acr (**2a**), Ade–C_5–Acr (**2b**), and Ade–C_6–Acr (**2c**) in H_2O–EtOH (95:5) acetate buffer (5×10^{-2} M, pH, 5.5). % H is computed for the 360–500-nm absorption band.

tative basis, following a methodology previously used in this laboratory. The absorptions of model compounds and references were recorded at various temperatures in the range 2.5–80 °C. The corresponding % H values were calculated and plotted against temperature (Figure 1). The most dramatic effects are observed in the adenine series. For Ade–C_3–Acr (**2a**), % H is high and remains constant over the temperature range examined (Bolte et al., 1982). However, for longer linking chains [n = 5, 6; Ade–C_5–Acr (**2b**) and Ade–C_6–Acr (**2c**)], the % H values are lower and increase linearly from 75 to 50 °C and reach a maximum asymptotic value at lower temperatures. A comparable behavior has been observed previously for other intercalating drugs studied in our laboratory (Bolte et al., 1979; Dêcout & Lhomme, 1983). Those parts of the curves where % H remains high and constant have been associated with totally folded conformations, while the decrease of % H corresponds to the "opening" (unfolding) of the system.

These observations lead us to conclude that all three Ade–C_n–Acr model molecules exhibit a degree of folding equal to 100% at the lowest temperatures. Correlatively, this means that the *% H values associated with 100% folding are strongly dependent on the length of the linking chain* between the chromophores. Comparable results are observed in the guanine and thymine series as well (Table I). The determination of the % H_{max} value allows us to have an estimate of the degree of folding for the systems (if we assume that the equilibrium can be described with the simple scheme involving two extreme limits: opened forms ⇌ stacked forms). The equilibrium constant K and the degree of folding (% R) can be calculated as

$$K = \frac{\text{opened forms}}{\text{stacked forms}} = \frac{\%\ H}{\%\ H_{max} - \%\ H}$$

$$\%\ R = \frac{\%\ H}{\%\ H_{max}} \times 100$$

The value of K for different temperatures can be used to calculate the thermodynamic parameters of the systems. By plotting the van't Hoff curves $\ln K = f(1/T)$, according to the relation $\Delta G = -RT \ln K = \Delta H - T\Delta S$, the following values are obtained: $\Delta S° = -140 \pm 20$ J mol^{-1} deg^{-1}, $\Delta H° = -50 \pm 10$ kJ mol^{-1} for Ade–C_5–Acr (**2b**); $\Delta S° = -150 \pm 25$ J mol^{-1} deg^{-1}, $\Delta H° = -55 \pm 10$ kJ mol^{-1} for Ade–C_6–Acr (**2c**).

Other intercalating drugs studied in our laboratory show comparable behavior. In the quinoline series (Bolte et al., 1977, 1979) for both Ade–C_3–Qui and Gua–C_3–Qui models (i.e., models in which the base Ade or Gua is linked to the 7-chloro-4-aminoquinoline ring of the drug chloroquine), we measured $\Delta H° = -37$ kJ mol^{-1} and $\Delta S° = -100$ J mol^{-1} deg^{-1}. In the psoralen series (Dêcout & Lhomme, 1983), for the Ade–C_3–8Pso model, the thermodynamic parameters were $\Delta H° = -30$ kJ mol^{-1} and $\Delta S° = -90$ J mol^{-1} deg^{-1}.

We also determined the influence of organic solvents like ethanol on the % H values. This type of solvent is well-known for its denaturing effects on nucleic acids. The models Ade–C_5–Acr (**2b**), Thy–C_5–Acr (**3b**), and Gua–C_5–Acr (**4c**) were examined. In all cases we observe a strong decrease of % H when the ethanol content increases. In neat ethanol, % H is small (0.5–3%). In this solvent, the stacking interactions disappear and the models exist essentially in their open forms. This behavior reflects the hydrophobic nature of the interactions involved in the complex between intercalating drugs and the nucleic acid bases.

^{1}H NMR Studies

Mutual interactions between aromatic moieties in compounds of the type base–C_n–Acr should be readily observable by ^{1}H NMR spectroscopy, since both nucleic bases and acridines exhibit shielding effects (Giessner-Prettre & Pullman, 1976a,b). If we compare the chemical shifts of the model compounds with those of the references Acr–C_6 (**5**) and base–C_3 (**6–8**), the folded conformations can be detected by the upfield shifts induced on the protons of the intramolecularly stacked molecules. The experimental shielding effects $\Delta\delta$ would reflect the proportion of folded molecules: $\Delta\delta = \delta$(reference) – δ(model). However, self-association of nucleic bases and acridine moieties induces upfield shifts as well. Consequently, we investigated the self-association phenomena exhibited by all moieties involved in the folding–unfolding process. This was done by measuring the concentration dependence of the aromatic proton chemical shifts, and the data were treated to extract the chemical shifts at infinite dilution (Dimicoli & Helene, 1973).

(*1*) *Self-Association of the Reference Molecules Ade–C_3, Thy–C_3, Gua–C_3, and Acr–C_3.* The proton signals for Ade–C_3 (**6**), Thy–C_3 (**7**), and Gua–C_3 (**8**) were not significantly altered on dilution of 10^{-2} M solutions to 10^{-4} M. This indicates the absence of self-association phenomena under these conditions. The very limited solubility for Acr–C_3 (**5**) did not allow the accurate determination of the self-association constant. Nevertheless, the large shielding of the chemical shifts in a narrow concentration range (2×10^{-4}–5×10^{-5} M) only permits us to estimate a value of the order of 400 L M^{-1} for K_{assoc}.

(*2*) *Self-Association of the Model Compounds.* (*a*) *Adenine Series.* The chemical shifts of the aromatic protons are strongly dependent on the concentration (Figure 2). In all cases (n = 3, 5, 6) the protons of the acridine moiety are deshielded when the concentration is decreased. The adenine protons (H-2A and H-8A) behave differently. For Ade–C_3–Acr they exhibit deshielding with dilution (Bolte et al., 1982). For longer linking chains, on the contrary, a marked shielding is observed, more pronounced for n = 6.

(*b*) *Thymine Series.* A comparable behavior is exhibited by all the thymine models, characterized by strong deshielding of the acridine protons when dilution increases. For Thy–C_6–Acr and with a minor amplitude for Thy–C_5–Acr the H-6T and methyl thymine protons are again unexpectedly

Table II: Differences $\Delta\delta_0$ between the Chemical Shifts δ_0 (ppm) Extrapolated to Zero Concentration for the Models and the Corresponding Reference "Half-Molecules"[a]

compound	H-1	H-3	H-4	H-5	H-7	H-8	H-2A	H-8A	H-6T	CH_3T	H-8G
Ade–C_3							8.30	8.22			
Thy–C_3									7.51	1.90	
Gua–C_3											7.74
Acr–C_3	7.69	7.67	7.78	7.82	7.51	8.39					
Ade–C_5–Acr	7.29	7.66	7.76	7.85	7.46	8.24	7.50	7.92			
Ade–C_6–Acr	7.40	7.67	7.78	7.83	7.46	8.23	7.74	7.92			
Thy–C_5–Acr	7.65	7.66	7.79	7.86	7.52	8.37			7.16	1.60	
Thy–C_6–Acr	7.66	7.66	7.77	7.84	7.49	8.36			7.29	1.65	
Gua–C_5–Acr	7.33	7.61	7.73	7.8	7.44	8.25					7.55
Gua–C_6–Acr	7.44	7.72	7.71	7.79	7.42	8.23					7.49

[a] $\Delta\delta_0 = \delta_0$(reference) $- \delta_0$(model); D_2O, sodium deuterioacetate buffer, 0.04 M, pD 5.6, 21 °C.

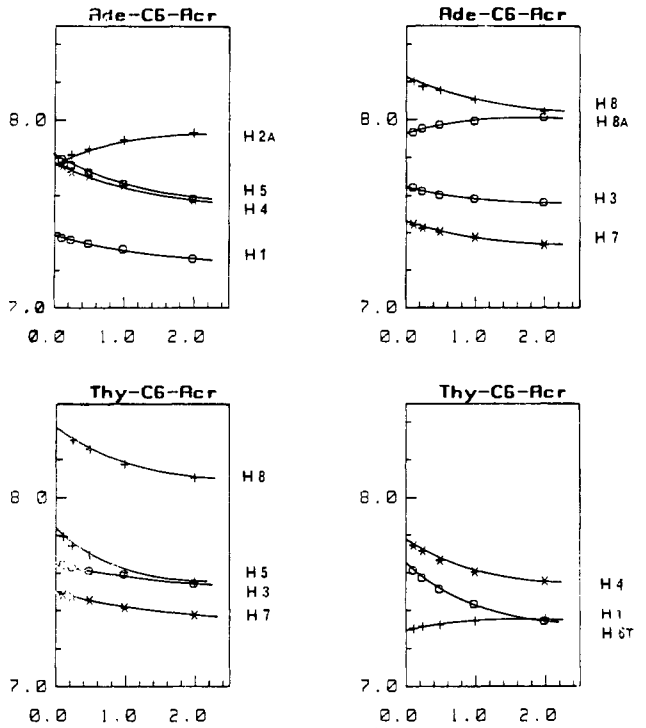

FIGURE 2: Concentration dependency (2×10^{-3}–1×10^{-4} M) for the proton chemical shifts of Ade–C_6–Acr and Thy–C_6–Acr in D_2O, 0.04 M sodium deuterioacetate buffer, pD 5.6, $T = 21$ °C (chemical shifts, δ; concentrations, 10^{-3} M).

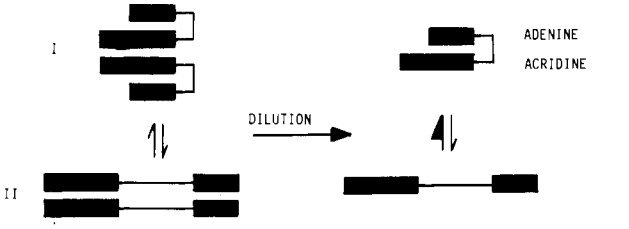

FIGURE 3: Schematic representation of the monomeric and dimeric species involved in the dilution process of models in water at 25 °C. At the monomeric stage the folded forms predominate. All dimeric species involve acridine–acridine contacts. For $n = 3$, I predominates; for $n = 6$, II predominates.

shielded (Figure 2). No such effect was observed for Thy–C_3–Acr (Bolte et al., 1982).

(*c*) *Guanine Series.* The very poor solubility of Gua–C_5–Acr and Gua–C_6–Acr could not allow the study over a wide range of concentrations. In the range 1×10^{-4}–3×10^{-6} M slight shielding is observed for all protons. No observable change can be detected below 3×10^{-6} M.

In those three series the concentration dependency of the chemical shifts with dilution affords by extrapolation the values at infinite dilution δ_0. However, the intermolecular association constants K_{assoc} cannot be extracted from those data by using the usual Dimicoli and Helene relationship (Dimicoli & Helene, 1973) due to the complexity of the process, which probably involves several types of aggregates. The deshielding of the acridine signals observed in all systems when dilution is increased is clear evidence of the presence of intermolecular stacking interactions involving the acridine rings (type I and/or type II aggregates; (Figure 3). The corresponding shielding of the base signals observed with longer linking chains ($n = 6$) is less clear. A possible interpretation is that type II aggregates predominate in solution in the latter case due to the chain–chain hydrophobic contribution, which increases with the length of the bridge. Dilution yields the monomer in its folded conformation for all models. In this process intermolecular base–base stacking in II is replaced by intramolecular base–acridine stacking in the folded monomer, with the result that the base proton signals undergo a larger shielding [the ring current of the base being weaker than the ring current of the acridine nucleus (Giessner-Prettre & Pullman, 1976a,b)].

(*3*) *Intramolecular Stacking.* The intramolecular ring–ring stacking was determined quantitatively by $\Delta\delta_0 = \delta_0$(reference) $- \delta_0$(model), the difference in the chemical shifts extrapolated to infinite dilution for the corresponding protons in the model and in the reference compounds (Table II).

In the adenine series, the strongest shielding is observed for the adenine H-2A and H-8A protons and for two protons of the acridine moiety, H-1 and H-8. The effect of chain lengthening is different for these four protons. This behavior has to be related to geometrical considerations, which will be discussed below.

In the thymine series, the effects on the thymine protons are important. On the contrary, the acridine protons are not markedly perturbed by the folding due to the small induced diamagnetic field exhibited by pyrimidines (Giessner-Prettre & Pullman, 1976a,b).

In the guanine series, the behavior is quite comparable to the Ade–C_n–Acr models. The shielding values measured are of the same order of magnitude.

(*4*) *Temperature Dependency of the Chemical Shifts.* The UV experiments have outlined the interest of a temperature study to compare the tendencies for different model molecules to stack intramolecularly. It was thus highly desirable to perform a comparable study by ^1H NMR spectroscopy. We thus determined the chemical shift differences $\Delta\delta_0$ at 92 °C to compare the values with those measured at 25 °C. Again, The δ_0 values must characterize the monomeric molecules in the absence of any intermolecular contribution. To evaluate the contribution of self-association at 92 °C, we examined the acridine molecule Acr–C_3, which is most prone to aggregate ($K \simeq 400\ M^{-1}$). Figure 4 plots the chemical shifts as a function of temperature measured at two concentrations, 2×10^{-3} and

Table III: Chemical Shift Differences $\Delta\delta_0$ Measured at 25 and 92 °C for the Model Compounds Thy–C_n–Acr **3a–c** and Ade–C_n–Acr **2a–c**

compound	T (°C)	H-1	H-8	H-2A	H-8A	H-6T	CH_3T
Thy–C_3–Acr (**3a**)	25[a]	0.07	0.07			0.38	0.44
	92[b]	0.08	0.07			0.33	0.35
Thy–C_5–Acr (**3b**)	25[a]	0.04	0.02			0.35	0.30
	92[b]	0.02	0.01			0.25	0.19
Thy–C_6–Acr (**3c**)	25[a]	0.03	0.03			0.22	0.25
	92[b]	−0.01	0.00			0.16	0.12
Ade–C_3–Acr (**2a**)	25[a]	0.48	0.22	0.75	0.21		
	92[b]	0.44	0.29	0.64	0.28		
Ade–C_5–Acr (**2b**)	25[a]	0.40	0.15	0.80	0.30		
	92[b]	0.25	0.16	0.51	0.26		
Ade–C_6–Acr (**2c**)	25[a]	0.29	0.16	0.56	0.30		
	92[b]	0.14	0.12	0.26	0.19		

[a] $\Delta\delta$(25 °C) = $\Delta\delta_0$(25 °C) = δ_0(reference) − δ_0(model); extrapolated values to zero concentration at 25 °C. [b] $\Delta\delta$(92 °C) = δ(92 °C, reference) − δ(92 °C, model); experimental values measured at 92 °C and 5×10^{-4} M.

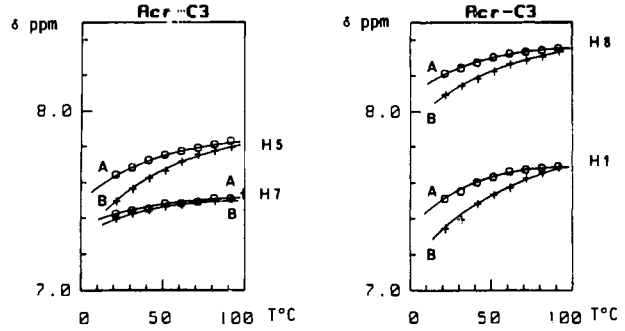

FIGURE 4: Influence of temperature on the chemical shifts of Acr–C_3 (D_2O, 0.04 M sodium deuterioacetate buffer, pD 5.6): (A) 5×10^{-4} M; (B) 2×10^{-3} M.

5×10^{-4} M. In both cases increasing the temperature leads to deshielding for all aromatic protons. This corresponds to the expected destruction of the acridine–acridine aggregates with temperature. The deshielding is more pronounced at the highest concentration, where aggregate percentage is higher. Quite interestingly, for a given proton the same δ_0 value is reached at 92 °C at the two concentrations, and these δ_0 values correspond to those determined by extrapolation to infinite dilution at 25 °C. This means total destruction of the aggregates at 92 °C. At this temperature the difference is only due to intramolecular stacking. Some of the most significant values are collected in Table III, along with the corresponding data determined at 25 °C. For all the systems considered, shielding effects remain important at high temperatures. Folded conformations are still predominant at 92 °C.

In the adenine series, for $n = 3$, shielding effects are almost independent of temperature. This corroborates the UV results and confirms the interpretation that the system is stacked to a 100% degree throughout the temperature range. For $n = 5$ and 6, shielding is smaller.

In the thymine series, for $n = 3$, the shielding effect is slightly decreased by temperature. This tendency is enhanced for longer linking chains ($n = 5$, 6).

The percentage of folded conformation (% R) at 92 °C (in which we assume 100% folding at 25 °C) can be estimated by

$$\% R = \frac{\Delta\delta(92\ °C)}{\Delta\delta_0(25\ °C)} \times 100$$

These % R values are compared (Table IV) with the UV spectrophotometry data, obtained by extrapolation of the curves % $H = f(T)$ at 92 °C. The values obtained by the different techniques are in good agreement.

(*5*) *Geometry of the Stacked Complexes.* In the case of Thy–C_n–Acr, the ring current of thymine is quite small and the acridine protons are virtually unshifted. Given this paucity of data, the geometry of the folded forms could not be established.

However, in the case of Ade–C_n–Acr models, comparison between the proton chemical shifts in Ade–C_n–Acr, Ade–C_3, and Acr–C_3 extrapolated to infinite dilution with the values calculated from the isoshielding curves of adenine and acridine established the geometries of the folded conformations, which are shown in Figure 5. Taking into account the restriction of the motion of the two rings, for a given model, only one stacked geometry gives a good fit between the experimental and the computed values. The folded forms are characterized (1) by superposition of the NH_2 group of adenine onto the positively charged nitrogen of acridine, (2) by a greater overlap of the ring bearing the methoxy group than the opposite one bearing the chlorine substituent, and (3) by a greater overlap of the adenine ring when the linking chain increases from $n = 3$ to $n = 6$.

Table IV: Comparative Values for the Degree of Folding (% R) at 92 °C of the Model Compounds Ade–C_n–Acr and Thy–C_5–Acr Calculated from UV[a] and ^{1}H NMR[b] Data

% R	Ade–C_3–Acr (**2a**)	Ade–C_5–Acr (**2b**)	Ade–C_6–Acr (**2c**)	Thy–C_5–Acr (**3b**)
UV[a]	100	75	50	70
^{1}H NMR[b]	100	70	50	65

[a] Calculated by the equation % R = 100[(% H)/(% H_{max})] with values extrapolated from the curves reported in Figure 1. [b] % R values were calculated separately for the H-1, H-2A, and H-8A protons in the adenine models and for the H-6T and CH_3T in the thymine series according to the equation % R = 100$\Delta\delta$(92 °C)/$\Delta\delta$(25 °C)]. From these data, we calculated for each model compound the average % R values, which are given in the table.

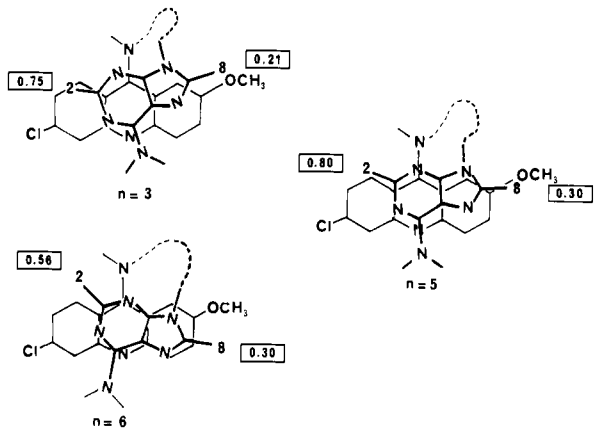

FIGURE 5: Proposed geometries for the stacked forms of Ade–C_n–Acr deduced from the comparison between the upfield shifts computed from isoshielding curves [$\Delta\delta$(comp)] and the experimental shifts [$\Delta\delta_0$(exp)] extrapolated to zero concentration.

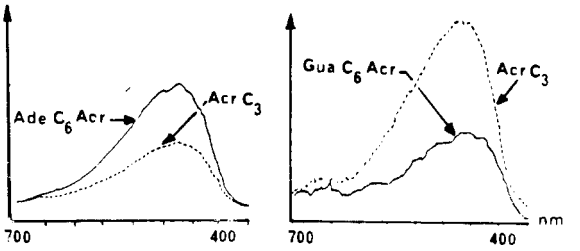

FIGURE 6: Emission fluorescence spectra (arbitrary units) measured between 350 and 750 nm (λ_{exc} = 360 ± 7 nm) for Ade–C_6–Acr, Gua–C_6–Acr, and Acr–C_3 in H_2O–EtOH (95:5), 8 × 10^{-5} M, 0.05 M acetate buffer, pH 5.5.

This overlapping phenomenon is also associated with continuous relative rotation of one ring upon the other. This latter process can be estimated quantitatively from the geometries indicated on Figure 5, if one defines a general axis for each aromatic moiety in the models (for example, the axis in the largest dimension). The increase of the length of the linking chain from n = 3 to n = 5 corresponds approximately to a 20° rotation between the two rings. With one more methylene in the bridge (n = 6) rotation occurs in the same direction with an angle of the same magnitude. These observations can be correlated with the results obtained by UV spectroscopy. The measured hypochromism values (% H) corresponding to totally folded systems were quite different for the different chain lengths (n = 3, % H = 20; n = 5, % H = 13; n = 6, % H = 7). This means that hypochromism is directly a function of the relative orientations of the adenine and acridine rings in the intramolecular complex. In the guanine series, similar effects were observed.

Fluorescence Studies

The fluorescence emission spectrum of quinacrine, when intercalated, is dramatically changed (Nastasi et al., 1976; Birks, 1976). In double-stranded DNA, the intensity of the fluorescence emitted by the bound dye is decreased as compared with the free one at the same concentration. In synthetic polynucleotides, the fluorescence emitted by intercalated quinacrine is strongly quenched by GC base pairs but is enhanced by AT base pairs. This behavior has not yet been explained. It has been proposed that four consecutive AT base pairs are necessary for increasing the fluorescence but only one GC base pair is able to quench it (Baldini et al., 1981).

The interest of the synthetic models base–C_n–Acr is their ability to show interactions between the intercalator and a single nucleic base. As a preliminary study, we considered the emission spectra of some base–C_n–Acr compounds and their reference compound Acr–C_3. The concentration ranges were 8 × 10^{-5} M for Acr–C_3 and (2.5–6.5) × 10^{-5} M for the models. We checked that in these conditions the Acr–C_3 spectrum was not altered by added nucleic base at the same concentration. In thymine and adenine models, the fluorescence of the acridine moiety is strongly enhanced by the stacking interactions. On the contrary, the guanine nucleus induces an important quenching by a factor of 4 (see Figure 6). The corresponding fluorescence quantum yields are shown in Table V.

Interactions with DNA

NMR and UV–visible studies have shown that all model compounds adopt folded conformations at 25 °C. The stability of these folded states depends upon both the nature of the base and the length of the linking chain, the largest being observed with Ade–C_3–Acr (**3**). It was then of interest to investigate to what extent folding can modulate DNA binding parameters,

Table V: Fluorescence Quantum Yields ϕ(F) Determined for the Base–C_n–Acr Compounds (n = 5, 6) and Acr–C_3 (λ_{exc} = 360 ± 7.5 nm; λ_{max} = 490 nm)

compound	ϕ(F) × 10^{-2}	ϕ(F, model)/ ϕ(F, Acr–C_3)
Thy–C_5–Acr (**3b**)	9	3
Thy–C_6–Acr (**3c**)	6	2
Ade–C_5–Acr (**2b**)	12	4
Ade–C_6–Acr (**2c**)	10.5	3.5
Gua–C_5–Acr (**4b**)	0.7	0.25
Gua–C_6–Acr (**4c**)	1	0.33
Acr–C_3 (**5**)	3	

Table VI: DNA Binding Parameters for Acr–C_3 and Model Compounds Determined in 25 mM Tris, pH 7, 0.1 M NaCl, and 0.2 mM EDTA

compound	K × 10^{-4} (M^{-1})	n (base pairs)
Acr–C3 (**5**)	6	1.8
Ade–C_3–Acr (**2a**)	0.45	2.5
Ade–C_5–Acr (**2b**)	3.4	1.9
Ade–C_6–Acr (**2c**)	6.8	1.2
Thy–C_3–Acr (**3a**)	2	2
Thy–C_3–Acr (**3b**)	4	2.5
Thy–C_6–Acr (**3c**)	6.5	2
Gua–C_5–Acr (**4b**)	2	2.5
Gua–C_6–Acr (**4c**)	8	0.5

i.e., K_a (association constant) and n (number of base pairs covered by the dye).

Both parameters were determined through competition experiments, with ethidium bromide used as the competitor. Experimental data were fitted according to the equations of Mac Ghee and Von Hippel (1974) as already described by Gaugain et al. (1978), yielding the values reported in Table VI.

All compounds except purine–C_6–Acr cover about two pairs, which is consistent with an excluded site binding. The smaller value of n for Ade–C_6–Acr (**2c**) and Gua–C_6–Acr (**4c**) suggests a more complex binding mode. Interestingly, this phenomenon occurs with both dyes, which are less prone to fold and are able to form type II aggregates. This might be related to the occurrence, in our experimental conditions, of additional external dye–dye stacking involving, e.g., the purines. Such behavior has also been encountered with acridine orange (Fredericq & Houssier, 1972).

With regard to the DNA affinities, compound Ade–C_3–Acr (**2a**), which adopts the most stable folded conformation, also elicits the lowest DNA affinity (K_a = 4.5 × 10^3 M^{-1}). The DNA affinity increases with the length of the linking chain, regardless of the nature of the base, to reach that of reference compound Acr–C_3 for n = 6. It should also be emphasized that with n = 3 or 5 the DNA affinity increases when a purine is replaced by a pyrimidine. It is thus clear that the more folded a compound is, the less it binds to DNA. However, the gap between the strongest and weakest DNA binding dyes is only 1 log unit, although the latter is always totally folded at 80 °C. This suggests a key role for entropic factors upon DNA binding such as desolvation, as suggested by conformational studies in ethanol or kinetics of an acridine trimer (Laûgaa et al., 1985).

CONCLUSIONS

We may cite the following as three important conclusions from the present work:

(1) UV and NMR spectroscopies, run at different temperatures, are remarkably complementary to analyze the conformational behavior of the acridine–base heterodimers. The degree of stacking, the preferred conformations, and the

geometries of the complexes could be determined in detail. The base–acridine stacking observed in the models is of the same nature as that found when acridine is intercalated in DNA, as revealed by the similarities of the UV spectra. The acridine–base interactions are strong in water, as evidenced by the high degree of folding of the molecules; they are hydrophobic in nature, as indicated by the decrease of the folding in organic solvents.

(2) The acridine–base heterodimers can be considered as spectroscopic models of the complex formed when acridine is intercalated in DNA. As the conformational behavior of the models could be established with great precision, it thus becomes possible to have precise knowledge of the spectroscopic modifications of the drug when complexed to a nucleotide base in a given geometry. This is illustrated in the case of the electronic absorption spectrum of acridine complexed to adenine. Hypochromism in the UV expressed by the "percent hypochromism" (% *H*) is generally considered as a measure of the interaction. % *H* is known to be dependent on the relative orientations of the chromophores (Warshaw & Tinoco, 1965; Cantor & Schimmel, 1980). However, quantitative experimental evidence for this dependency is largely missing. We show in the acridine–adenine series the dramatic influence of the geometry upon the amplitude of % *H*. The acridine–base dimers are also models for fluorescence spectroscopy of acridine intercalated in DNA; both adenine and thymine induce fluorescence enhancement, while the guanine ring quenches the fluorescence emission.

(3) The base–acridine dimers are DNA-binding agents. All the molecules include in their structure the intercalator 9-aminoacridine. We show that the degree of binding of this drug to DNA can be modulated according to the nature of the base and the length of the linking chain by which it is substituted. These molecules are now under study for their interactions with DNA containing apurinic sites (Constant et al., 1988).

Registry No. **2a**, 79953-24-5; **2b**, 103061-92-3; **2c**, 103061-94-5; **3a**, 79953-25-6; **3b**, 84889-92-9; **3c**, 103061-91-2; **4b**, 103083-41-6; **4c**, 103083-42-7; **5**, 79953-28-9.

REFERENCES

Baldini, G., Doglia, S., Sassi, G., & Lucchini, G. (1981a) *Int. J. Biol. Macromol. 3*, 248.

Baldini, G., Doglia, S., Dolci, S., & Sassi, G. (1981b) *Biophys. J. 36*, 465.

Birks, J. B. (1976) *Natl. Bur. Stand. (U.S.), Sect. A 80*, 389.

Bolte, J., Demuynck, C., & Lhomme, J. (1976) *J. Am. Chem. Soc. 98*, 613.

Bolte, J., Demuynck, C., & Lhomme, J. (1977a) *J. Med. Chem. 20*, 106.

Bolte, J., Demuynck, C., & Lhomme, J. (1977b) *J. Med. Chem. 20*, 1607.

Bolte, J., Demuynck, C., Lhomme, J., Fournie-Zaluski, M. C., & Roques, B. P. (1979) *Biochemistry 18*, 4928.

Bolte, J., Demuynck, C., & Lhomme, J. (1980) *Bull. Soc. Chim. Fr.*, 316.

Bolte, J., Demuynck, C., Lhomme, M. F., Lhomme, J., Barbet, J., & Roques, B. P. (1982) *J. Am. Chem. Soc. 104*, 760.

Browne, D. T., Eisinger, J., & Leonard, N. J. (1968) *J. Am. Chem. Soc. 90*, 7302.

Cantor, C. R., & Schimmel, P. R. (1980) in *Biophysical Chemistry*, Vol. 2, Freeman, San Francisco.

Cohn, W. E., Leonard, N. J., & Wang, S. Y. (1974) *Photochem. Photobiol. 19*, 89.

Constant, J. F., Carden, B. M., & Lhomme, J. (1985) *J. Heterocycl. Chem. 22*, 1035.

Constant, J. F., Fahy, J., & Lhomme, J. (1987) *Tetrahedron Lett. 28*, 1777.

Constant, J. F., O'Connor, T. R., Lhomme, J., & Laval, J. (1988) *Nucleic Acids Res. 16*, 2691.

Dêcout, J. L., & Lhomme, J. (1981) *Tetrahedron Lett. 22*, 1247.

Dêcout, J. L., & Lhomme, J. (1983) *Photochem. Photobiol. 37*, 155.

Dêcout, J. L., Huart, G., Lhomme, J., Courseille, C., & Hospital, M. (1984) *Nouv. J. Chim. 8*, 433.

Devoe, H., & Tinoco, J. (1962) *J. Mol. Biol. 4*, 518.

Dimicoli, J. L., & Helene, C. (1973) *J. Am. Chem. Soc. 95*, 1036.

Fornasiero, D., & Kurucsev, T. (1985) *Biophys. Chem. 23*, 31.

Fredericq, E., & Houssier, C. (1972) *Biopolymers 11*, 2281.

Gaugain, B., Barbet, J., Oberlin, R., Roques, B. P., & Le Pecq, J. B. (1978) *Biochemistry 17*, 5078.

Georghiou, S. (1977) *Photochem. Photobiol. 26*, 59.

Giessner-Prettre, C., & Pullman, B. (1976a) *Biochem. Biophys. Res. Commun. 70*, 578.

Giessner-Prettre, C., & Pullman, B. (1976b) *C. R. Hebd. Seances Acad. Sci., Ser. D 283*, 675.

Hahn, F. E. (1978) in *Antibiotics* (Corcoran, J. W., & Hahn, F. E., Eds.) Vol. III, p 203, Springer-Verlag, Berlin.

IUPAC–IUB Commission (1970) *Biochemistry 9*, 4022.

Krey, A. K., & Hahn, F. E. (1974) *Mol. Pharmacol. 10*, 686.

Krey, A. K., & Hahn, F. E. (1975) *Naturwissenschaften 62*, 99.

Kubota, Y., & Motoda, Y. (1980) *Biochemistry 19*, 4189.

Laûgaa, P., Markovits, J., Delbarre, A., Le Pecq, J. B., & Roques, B. P. (1985) *Biochemistry 24*, 5567.

Leonard, N. J. (1979) *Acc. Chem. Res. 12*, 423.

Leonard, N. J., & Lambert, R. F. (1969) *J. Org. Chem. 34*, 3240.

Leonard, N. J., & Ito, K. (1973) *J. Am. Chem. Soc. 95*, 4010.

Mac Ghee, J. D., & Von Hippel, P. H. (1974) *J. Mol. Biol. 86*, 469.

Nastasi, M., Morris, J. M., Rayner, D. M., Seligy, V. L., Szabo, A. G., Williams, D. F., Williams, R. E., & Yip, R. W. (1976) *J. Am. Chem. Soc. 98*, 3979.

Patel, D. J. (1977) *Biopolymers 16*, 2739.

Thompson, P. E., & Werbel, L. M. (1972) in *Antimalarial Agents*, Academic, New York.

Waring, M. J. (1970) *J. Mol. Biol. 54*, 247.

Waring, M. J. (1975) *Chem. Ind. (London)*, 105.

Warshaw, M. M., & Tinoco, I. (1965) *J. Mol. Biol. 13*, 54.